Optimization of *S. aureus* dCas9 and CRISPRi Elements for a Single Adeno-Associated Virus that Targets an Endogenous Gene

Jon R. Backstrom,[1] Jinsong Sheng,[1] Michael C. Wang,[2] Alexandra Bernardo-Colón,[1] and Tonia S. Rex[1,2]

[1]Vanderbilt Eye Institute, Vanderbilt University Medical Center, Nashville, TN 37232, USA; [2]Department of Ophthalmology & Visual Sciences, Vanderbilt University School of Medicine, Nashville, TN 37232, USA

The power of CRISPRi to decrease targeted gene expression for clinical applications has been inhibited by delivery challenges. Existing constructs are too large to fit within the ~4.7 kb packaging size limitation of adeno-associated virus (AAV), the only FDA approved viral vector for clinical use. Therefore, we optimized CRISPRi components to generate a single AAV vector that contains all functional elements and effectively knocks down expression of an endogenous gene *in vivo*. First, we increased nuclear targeting of *Staphylococcus aureus* deactivated Cas9 (SadCas9) 4-fold by using a helical linker and the *c-Myc* nuclear localization signal. Second, we identified an amino-terminal Krüppel associated box (KRAB) construct as the most effective in decreasing expression of target genes *in vitro*. Third, we optimized promoters for guide RNA and evaluated mini-promoters for expression of KRAB-SadCas9 in liver cells. Our final construct decreased protein convertase subtilisin/kexin type 9 (*Pcsk9*) mRNA and secreted protein 5-fold *in vitro*. The corresponding AAV2/8 vector was localized in nuclei of liver cells and decreased *Pcsk9* mRNA and serum protein levels by 30% *in vivo*. This single AAV approach provides a potential clinically translatable method for decreasing targeted gene transcription by CRISPRi *in vivo*.

INTRODUCTION

Catalytically inactive Cas9 (dCas9) fused to the transcriptional repression domain KRAB has the potential to be a clinically relevant tool if delivered in the relatively cell-type selective, non-replicative, and clinically safe adeno-associated virus (AAV).[1–3] Due to the ~4.7 kb packaging size limitation of AAV, the relatively small *Staphylococcus aureus* deactivated Cas9 (SadCas9) is a good candidate for this approach. However, it is still 3.2 kb. The current gold standard for delivery of functional CRISPR interference (CRISPRi) machinery developed by the Gersbach group requires two AAV particles: one with SadCas9-Krüppel associated box (KRAB) and the other with a U6 polymerase promoter driving expression of a single guide RNA (sgRNA).[4] Transduction of the liver with this dual AAV achieved impressive knock-down of serum protein convertase subtilisin/kexin type 9 (Pcsk9).

Unfortunately, AAV is a relatively inefficient virus for transducing many cells *in vivo* and the likelihood of getting both vectors in suffi-

cient numbers of relevant cells for treatment efficacy in more complex tissues is very low (for review see Li and Samulski[5]). One previous study packaged the components of CRISPR activation (CRISPRa) into a single AAV and was successful in activating expression of an exogenous, overexpressed target.[6] Our study extends this previous work by optimizing nuclear targeting of Cas9 and successfully knocking down expression of an endogenous gene using a sgRNA both *in vitro* and *in vivo*.

CRISPR-based studies, whether gene editing (CRISPR) or epigenetic modification through interference (CRISPRi) or activation (CRISPRa) of gene expression typically rely on the high expression-level CMV promoter. Nonetheless, CMV is too large (~700 bp) to include in a functional CRISPRi or CRISPRa construct for packaging in AAV, which is the only FDA-approved viral vector. The downside is that selecting either a general or more tissue-selective promoter that is smaller (<370 bp) would likely result in lower mRNA levels relative to cytomegalovirus (CMV). We reasoned that although levels attained with CMV are probably more than is required for functional responses, significantly lower protein levels would require optimizing nuclear targeting, the location of KRAB within *Staphylococcus aureus* dCas9 (SadCas9), and the promoter for sgRNA. Here we report the generation of a complete CRISPRi construct that was packaged into a single AAV. Subsequent modifications of this optimized CRISPRi construct for other studies would entail selecting a <370 bp promoter that is active in the desired cell-type and the appropriate gRNA. In summary, we optimized SadCas9 nuclear targeting and KRAB fusion, and promoter size and selection to result in a single AAV vector that contains all functional CRISPRi components. As proof-of-concept we tested the same *Pcsk9* gRNA as used by the Gersbach group.[4] We then packaged our construct into liver-tropic AAV2/8 and demonstrated nuclear localization of KRAB-SadCas9 (N-KRAB) in liver cells and knock-down of *Pcsk9*.

Table 1. Effects of Linkers (GR or EA) and Nuclear Localization Signals (SV40 or myc) on the Distribution of SadCas9 in Transiently Transfected ARPE-19 Cells

SadCas9 Construct[a]	% Nuclear[b]
SadCas9-SV40	5.1 ± 0.8
SadCas9-GR-SV40	6.7 ± 1.1
SadCas9-EA-SV40	9.6 ± 3.6
SadCas9-myc	7.9 ± 0.3
SadCas9-GR-myc	14.9 ± 1.2
SadCas9-EA-myc	27.0 ± 2.8[c]

[a]Linker sequences of the 15-amino acid GR is [(GGGGS)₃] and the 17-amino acid EA is [A(EAAAK)₃A].

[b]Determined from dividing the number of cells with nuclear SadCas9 by the total number of immunolabeled cells. At least 250 cells were counted per experiment and the results are presented as the mean ± SD of three independent experiments.

[c]p = 0.0003 from one-way ANOVA followed by the Dunnett post-hoc multiple comparison test.

RESULTS

Optimization of SadCas9 Nuclear Targeting

We first directly addressed nuclear localization of SadCas9 using combinations of linkers and nuclear localization signals in the human retinal pigmented epithelium cell line, ARPE-19. The commonly used combination of a flexible 15 amino acid, glycine-rich (GR) linker and the SV40 nuclear localization signal (NLS) at the carboxyl-terminus of SadCas9 resulted in only 6.7% ± 1.1% of transfected cells with nuclear SadCas9 (Table 1). However, a rigid helical 17 amino acid linker[7] before the *c-Myc* (myc) NLS increased nuclear localization of SadCas9 4-fold (27.0% ± 2.8%, p = 0.0003). Therefore, the combination of a helical linker (EA linker) and myc NLS was used in all subsequent SadCas9 constructs.

The carboxyl-terminus of SadCas9 is juxtaposed against the topoisomerase TOPO domain.[8] Since Arg[215] (*circle* above sequences in Figure 1A) of SadCas9 interacts with the non-target strand protospacer adjacent motif (PAM),[8] we examined whether truncations downstream of Arg[215] further enhanced the percentage of cells with nuclear SadCas9 while decreasing the size of SadCas9. Relative to wild-type (WT) SadCas9, removing 18 amino acids (Δ1036) decreased the percentage of cells with nuclear SadCas9 2-fold (p = 0.008) whereas removing an additional 3 amino acids (Δ1033) did not affect trafficking (Figure 1A). However, the loss of 21 amino acids (Δ1,033) resulted in decreased protein levels relative to WT SadCas9 (Figure 1B). Notably, these cell lines were generated using a Sleeping Beauty transposon system[9,10] and expression of SadCas9 was under the control of a Tet-ON promoter.[11] This allowed us to quickly survey a polyclonal population of cells with protein expression limited by the addition of doxycycline (Dox). WT SadCas9 was detected exclusively in nuclei of Dox-treated cells (Figure 1C), but the pattern was more reminiscent of nucleoli than nucleoplasm. We therefore evaluated whether addition of KRAB would alter the nuclear distribution of SadCas9.

KRAB Placement within SadCas9

The accessibility of the SadCas9 amino-terminus was examined using antibody-antigen binding as a model for transcription factor protein-protein interactions. Either 1 amino acid (T) or the commonly used 7-amino acid flexible, GS linker (GGSGGGS) was used to separate the FLAG-tag from the amino-terminus of SadCas9. Co-labeling with antibodies against Cas9 (red) and FLAG (green) revealed increased availability of the amino-terminal "spatial domain" of SadCas9 with the GS linker (Figure 2A). The GS linker was therefore included between KRAB and SadCas9 in the amino-terminal (N-KRAB) construct. Additional constructs with KRAB positioned at either an internal site (I-KRAB) or the carboxyl-terminus (C-KRAB) of SadCas9 were used to generate cell lines. The cellular distribution of N-KRAB (Figure 2B) and C-KRAB (data not shown) were exclusively nuclear, and importantly, consistent with a nucleoplasmic pattern in contrast to the nucleolar-like pattern of SadCas9 (Figure 1C). These results establish that inclusion of KRAB changes the nuclear localization of SadCas9. In contrast, I-KRAB was below the level of detection in immunocytochemistry experiments. A comparison of expressed protein revealed similar levels of N-KRAB and C-KRAB, but dramatically lower levels of I-KRAB (Figure 2C); I-KRAB was therefore not included in subsequent functional studies. The unexpected finding that N-KRAB migrated to a position between SadCas9 and C-KRAB (Figure 2C) warranted further examination.

Analysis of N-KRAB

Experiments were performed to assess whether N-KRAB was being translated at a downstream methionine, the KRAB domain was being cleaved, or alternatively, N-KRAB displayed an anomalous migration pattern (Figure S1). Potential downstream translation start sites were evaluated with SadCas9 constructs that were truncated (-tr) at Ile[311] to provide accurate determination of mass on blots (Figure S1A). The constructs had FLAG-tags at the carboxyl-terminus to allow detection of the Cas9 proteins with antibodies against FLAG, as well as Sa Cas9. N-KRAB-tr is predicted to be 8 kDa larger than SadCas9-tr but the results from blots document a 4 kDa difference. Mutation of Met[34] within KRAB and Met[71] at the beginning of SadCas9 (M34A/M71A) did not result in an increased size (Figure S1A), establishing that translation is not occurring at a downstream site. The possibility that N-KRAB is cleaved within the KRAB domain was examined with a hemagglutinin (HA)-tag at the amino-terminus of full-length SadCas9 (HA-SadCas9) and N-KRAB (HA-N-KRAB; Figure S1B). Mouse anti-Cas9 immunoprecipitates from transiently transfected cells were probed with rabbit antibodies against Cas9 (top panel) or HA-tag (bottom panel). A larger apparent mass of HA-N-KRAB relative to HA-SadCas9 was observed with both antibodies, which is consistent with an intact KRAB domain, at least within a subpopulation of HA-N-KRAB molecules. Finally, transfected cells labeled with anti-HA (Figure S1C) confirm that a population of full-length HA-N-KRAB molecules with a functional myc-NLS reaches the nucleus. Together, the results were consistent with an anomalous migration pattern of N-KRAB, but we cannot rule out the possibility that the presence of an HA-tag in some of these studies altered cleavage of KRAB. Nonetheless, N-KRAB and

Rb anti-Sa Cas9   DAPI (nuclei)   Merged
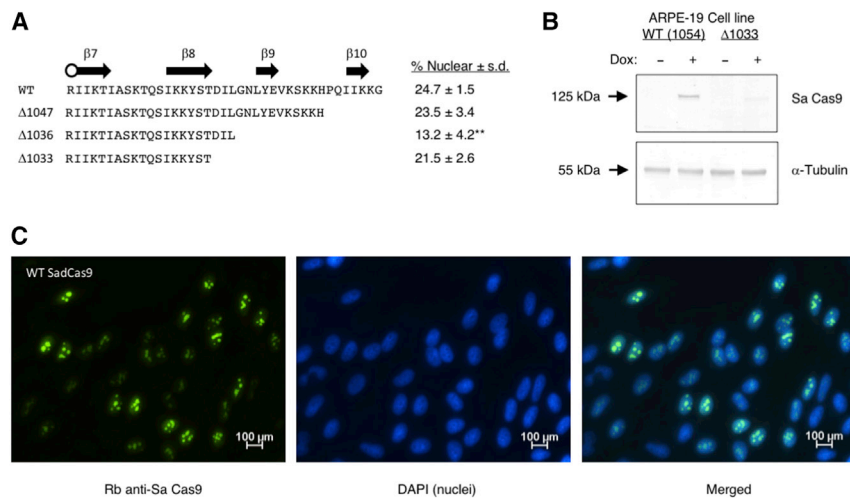
Figure 1. Analysis of SadCas9

(A) Effect of carboxyl-terminal truncations on nuclear targeting of SadCas9. All constructs had the EA linker and the myc-NLS at the extreme carboxyl-terminus (Table 1). The sequence begins at Arg[1015] ("O") and locations of β-structure are marked above the protein sequence (adapted from Nishimasu et al.[8]). Asterisks (**) denote a significant difference ($p < 0.01$) between WT and Δ1,036 SadCas9. (B) Blot of extracts from ARPE-19 cell lines expressing WT or Δ1033 SadCas9 grown in the absence or presence of 5 μg Dox/mL. (C) ARPE-19 polyclonal cell line expressing WT SadCas9 (5 μg Dox/mL) displayed punctate labeling (green) within nuclei (blue).

C-KRAB were examined in functional studies, where CRISPRi activity of N-KRAB constructs would establish that its unusual migration pattern in gels was not due to a loss of KRAB function.

CRISPRi Activity against VIMENTIN

The ability of the SadCas9 constructs with KRAB to decrease gene expression was tested in ARPE-19 cell lines with *VIMENTIN* as the target. Polyclonal cell lines expressing N-KRAB or C-KRAB under control of the Tet-ON promoter were transiently transfected with a bicistronic plasmid composed of the SV40 promoter driving expression of ZsGreen and the U6 promoter driving expression of sgRNA (Figure S2A). Example fluorescence images of N-KRAB cells expressing either non-targeting (NT) or *VIMENTIN* (C5) gRNA labeled with anti-vimentin are shown in Figure S2B. Vimentin immunofluorescence intensity (red channel) was measured in ZsGreen-positive cells (green channel) with the application ImageJ. Red fluorescence was measured in at least 100 ZsGreen-positive cells and presented as the mean ± SD of fluorescence per cell. An analysis of 5 vimentin gRNAs revealed that co-expression of the C5 gRNA plasmid resulted in a significant 2-fold decrease in vimentin immunofluorescence in the N-KRAB cell line (Figure S2C; $p = 0.02$) relative to the NT gRNA. However, there was no significant difference with the C-KRAB cell line expressing the same C5 gRNA (Figure S2D). Bicistronic plasmids with the 7SK promoter provided identical results as the U6 promoter.[1] Therefore, additional cell lines were generated with either SadCas9, N-KRAB, or C-KRAB together with the 7SK promoter driving expression of the vimentin C5 gRNA. Examination of immunoreactive vimentin from the SDS-soluble fraction of each cell line (Figure S2E) revealed that only the N-KRAB cell line decreased vimentin protein levels 2-fold (Figure S2F; $p = 0.0004$). These results show that N-KRAB was a more effective CRISPRi construct than C-KRAB against *VIMENTIN*.

CRISPRi Activity against Pcsk9

The dual AAV system has been shown to decrease levels of serum Pcsk *in vivo*.[4] We therefore evaluated the CRISPRi activities of N-KRAB and C-KRAB using the same gRNA (gRNA2).[4] Tet-ON plasmids with the U6 promoter driving expression of non-targeting (NT) or *Pcsk9* gRNA were stably expressed in mouse liver AML-12 cells and treated with 5 μg Dox/mL of serum-free media. Similar levels of SadCas9 proteins were detected on blots from cell extracts (Figure 3A) and exclusive nuclear labeling (Figure 3B) was detected in the cell lines that express N-KRAB (left panel) or C-KRAB (right panel) along with *Pcsk9* gRNA. However, SadCas9 displayed the same punctate, nucleolar-like labeling (data not shown) as in the ARPE-19 cell lines (Figure 1C). Supernatant from cells grown in 5 μg Dox/mL of serum-free media were subjected to a Pcsk9 ELISA. Cells expressing SadCas9 alone showed a significant ($p = 0.006$) 2-fold reduction in secreted Pcsk9 levels relative to parental AML-12 cells (Figure 3C). A similar reduction was observed for N-KRAB(NT) or C-KRAB(NT). A further 3-fold and 1.5-fold reduction in secreted Pcsk9 was observed for N-KRAB(*Pcsk9*) and C-KRAB(*Pcsk9*) but only N-KRAB(*Pcsk9*) was significant ($p = 0.02$). However, the CRISPRi activity of C-KRAB(*Pcsk9*) was close to being significant ($p = 0.06$) when compared to SadCas9. Nonetheless, since N-KRAB decreased expression of both Pcsk9 and vimentin, N-KRAB was chosen as the model CRISPRi construct.

Analysis of U6 and 7SK Promoters

Whereas no differences between the U6 and 7SK promoter were detected for the vimentin experiments with ARPE-19 cells, a significant difference was observed from AML-12 cell lines. For these experiments, the negative control was a gStop gRNA composed of 6-"T"s, which effectively terminates transcription of both promoters.[12] Thus, these experiments could be considered as plus or minus guide RNA with the only other difference being the U6 or 7SK promoter. Cells were treated with 2 μg Dox/mL of serum-free media for 3 days. The cell lines expressed similar levels of N-KRAB protein (Figure 4A) and mRNA (Figure 4B). The U6(*Pcsk9*) construct decreased Pcsk9 mRNA 3-fold (Figure 4C; $p = 0.0006$) and secreted Pcsk9 3.5-fold (Figure 4D; $p = 0.0001$) relative to the U6(gStop) construct. In contrast, the 7SK(*Pcsk9*) construct did not significantly decrease Pcsk9 mRNA (Figure 4C), but significantly decreased secreted Pcsk9 1.5-fold (Figure 4D; $p = 0.008$) relative to 7SK(gStop). Since the U6 promoter displayed a 2.5-fold decrease in secreted Pcsk9
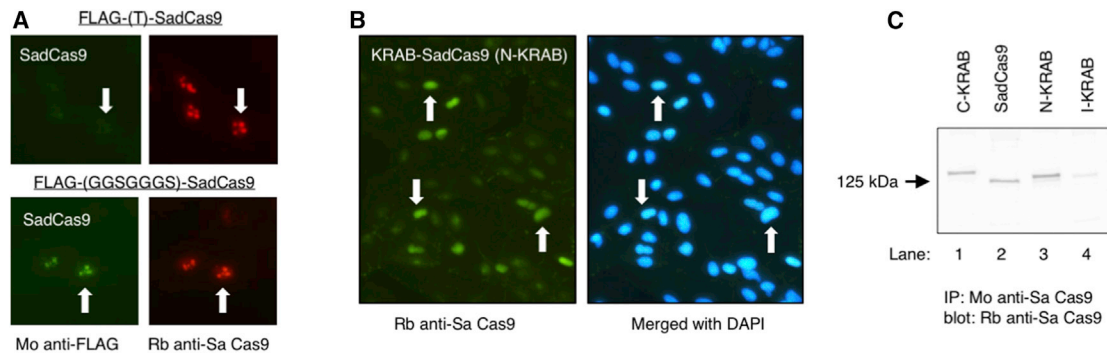
Figure 2. Analysis of SadCas9 Constructs with the Transcriptional Repression KRAB Domain

(A) The FLAG-tag was used to examine accessibility of the amino-terminal "domain" of SadCas9. Immunoreactive FLAG was barely detected with a single threonine residue between FLAG and SadCas9 (upper left panel) but was greatly enhanced with the 7-amino acid GS linker (lower left panel) and co-localized with imunoreactive SadCas9 (lower right panel). Therefore, the GS linker was used for the KRAB-SadCas9 (N-KRAB) construct. (B) Nuclear localization of N-KRAB in an ARPE-19 cell line that was treated with 5 μg Dox/mL. (C) Blot of immunoreactive SadCas9 proteins from the ARPE-19 cell lines. The N-KRAB construct migrated to a position between C-KRAB (lane 1) and SadCas9 at ~125 kDa (lane 3). The internal KRAB (I-KRAB) construct displayed significantly lower protein levels than the other constructs and was only detected by immunoprecipitation.

relative to the 7SK promoter (Figure 4D; p = 0.002), the U6 promoter was used in subsequent CRISPRi constructs.

Analysis of Promoters for N-KRAB

The remaining element for the design of the AAV plasmid was the promoter to drive expression of N-KRAB. For these experiments in AML-12 cell lines, the TET-On promoter was replaced with the general EF-1α promoter or more hepatocyte-specific combinations of enhancers and promoters.[13] The size of the enhancers and promoters used for these studies is shown in Table 2. Importantly, these plasmids contain all functional CRISPRi components and are within the size limitation of AAV packaging. Although inclusion of the CMV promoter exceeds the 4.7 kb AAV limit, it was used with gRNA for Pcsk9 or gStop as the positive and negative controls, respectively. The results showed that all tested promoters displayed 5- to 16-fold

lower levels of N-KRAB mRNA relative to CMV (Figure 5A). However, the EF-1α and the albumin enhancer/α1-antitrypsin (Alb-AAT) promoters were as effective as CMV in decreasing levels of Pcsk9 mRNA (5-fold, Figure 5B) and secreted protein (5-fold, Figure 5C). A diagram of the elements used to generate the 4.7 kb (including ITRs) AAV plasmids is shown in Figure 6A.

In Vivo Efficacy of AAV8.Pcsk9CRISPRi

Male mice were injected into the tail vein with AAV2/8 viruses and sacrificed 3 weeks later. RNA from liver was used to measure levels of N-KRAB and Pcsk9 mRNA and serum was collected to measure levels of Pcsk9 protein. Viruses with either the EF-1α or Alb-AAT promoter along with *Pcsk9* gRNA were evaluated for levels of N-KRAB mRNA from livers (Figure 6B). At doses of 2×10^{11} vg/mouse, the ΔCt values obtained from the Alb-AAT promoter virus
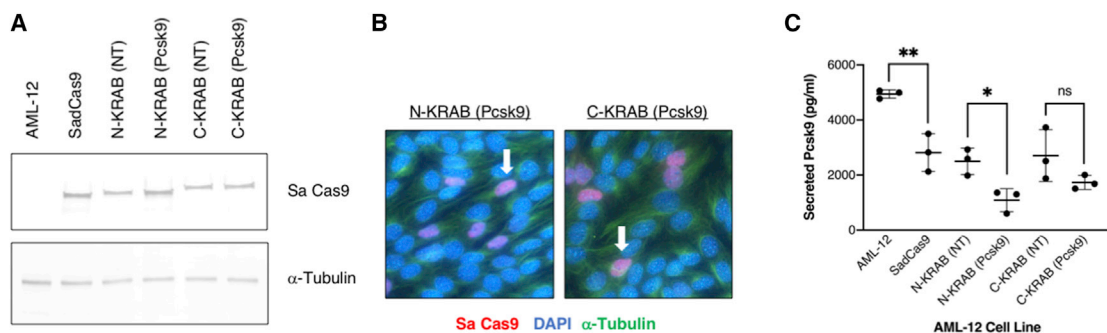
Figure 3. CRISPRi Activity Against the Secreted Protein Pcsk9

(A) Blot of soluble extracts from parental AML-12 mouse liver cells and cell lines expressing SadCas9, N-KRAB, or C-KRAB treated with 5 μg Dox/mL. The N-KRAB and C-KRAB constructs co-expressed U6-driven non-targeting (NT) or *Pcsk9* gRNA. (B) Both N-KRAB and C-KRAB were localized exclusively in the nucleus. Results in (A) and (B) are representative of two independent experiments. (C) Levels of Pcsk9 from the supernatant of cells. Relative to parental cells, cells with SadCas9 decreased Pcsk9 levels 2-fold (**p < 0.01). A comparison of NT versus *Pcsk9* gRNA revealed a significant difference (*p < 0.05) for N-KRAB, but not C-KRAB. The results (mean ± SD) are representative of three independent experiments.
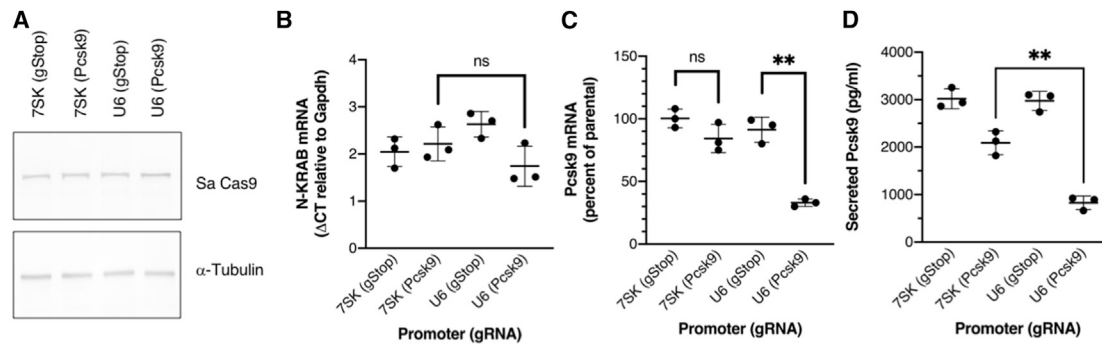
Figure 4. Comparison of 7SK and U6 Promoters Driving Expression of gRNA

AML-12 cell lines expressing N-KRAB and either 7SK or U6 promoters were treated with 2 μg Dox/mL for 3 days. (A) Blot of soluble protein from cell lines probed with antibodies against Sa Cas9 (top panel) or α-tubulin (bottom panel). The results are representative of two independent experiments. (B) Analysis of mRNA levels for N-KRAB relative to *Gapdh* [ΔCt = (Ct SadCas9) – (Ct Gapdh)]. (C) Levels of *Pcsk9* mRNA relative to parental cells. The U6 promoter and *Pcsk9* gRNA reduced levels of *Pcsk9* mRNA 3.5-fold relative to gStop (**p < 0.01), whereas there was no difference for the 7SK promoter. (D) Quantitation of Pcsk9 protein from the cell supernatants. A comparison between promoters with gStop gRNA was not significant, whereas promoters with *Pcsk9* gRNA revealed that the U6 promoter decreased Pcsk9 levels 2.5-fold relative to the 7SK promoter (**p < 0.01). The results (mean ± SD) presented in (B)–(D) are representative of three independent experiments.

corresponded to 12.1 ± 2.7-fold higher levels of N-KRAB mRNA relative to the EF-1α promoter virus (p < 0.0001). A 4-fold decrease in the dose of the Alb-AAT promoter virus to 5×10^{10} vg/mouse resulted in a similar 3.9-fold lower level of N-KRAB mRNA (p = 0.006). In contrast, a 2-fold increase to 4×10^{11} vg/mouse resulted in a trend toward lower levels of N-KRAB mRNA. We therefore evaluated the functional effects of AAV8 Alb-AAT viruses with either *Pcsk9* or gStop gRNA at a dose of 2×10^{11} vg/mouse. An analysis of Pcsk9 mRNA from livers revealed that the *Pcsk9* gRNA produced a 32% decrease in Pcsk9 mRNA relative to the virus with the gStop gRNA (Figure 6C; p = 0.0014). Similarly, the virus with *Pcsk9* gRNA reduced levels of serum Pcsk9 protein 27% relative to the virus with gStop gRNA (Figure 6D; p = 0.013). Finally, we examined immunoreactive N-KRAB in liver sections prepared from mice injected with either virus (Figure 6E, top panels) or PBS (bottom panels). Virally transduced livers displayed predominant nuclear labeling of N-KRAB that was above the level of control livers.

DISCUSSION

Targeting of CRISPR constructs to the nucleus has historically utilized one[14,15] or two[4] copies of the SV40 nuclear localization signal (NLS) along with an additional nucleoplasm-targeting sequence.[4,15] The lack of reports that document functionality of these targeting sequences is surprising. We therefore evaluated the effectiveness of NLS-targeting with a single SV40 or *c-Myc* NLS. We report that a single *c-Myc* NLS, along with a critical helical peptide, provide efficient nuclear localization of our N-KRAB CRISPRi construct both *in vitro* and *in vivo*.

Our finding that SadCas9 localizes to nucleolar-like structures in two different cell types was unexpected. Interestingly, SadCas9 has two potential nucleolar localization motifs within the bridge-helix domain. The first motif 51-KRxxxRxxRxR-61 has homology with Influenza A virus nonstructural protein 1 (NS1A)[16] and the second

motif 55-RR(I/L)xxxR-61 has homology with a subnuclear targeting arginine domain (STAD).[17] However, K51A/R52A/R55A/R56A mutations did not alter the nuclear pattern of SadCas9 immunoreactivity (data not shown). We hypothesized that co-expression of sgRNA within the same plasmid as SadCas9 would alter the distribution of SadCas9 to a nucleoplasmic location. Inclusion of the prototypic non-targeting (NT) gRNA found in most Cas9 plasmids did not alter the distribution of SadCas9 in ARPE cell lines (data not shown). This provides a cautionary note for *S. aureus* Cas9 CRISPR editing of nucleoplasmic genes as proper localization would likely result in efficient gene editing. We cannot rule out the possibilities that other gRNAs would provide nucleoplasmic localization or Cas9 is trafficked differently than catalytically inactive dCas9. Further investigation is clearly required to establish the mechanism of SadCas9 nucleolar-like localization. Fortunately, inclusion of KRAB at either the amino- or carboxyl-terminus of SadCas9 resulted in nucleoplasmic localization of the CRISPRi constructs.

The position of KRAB within SadCas9 was examined in three locations. Addition of KRAB at an internal site between Glu[277] and Leu[297], a region that lacks contact points with sgRNA,[8] resulted in low protein levels, which is likely due to protein instability. We therefore focused on constructs with KRAB at either the amino-terminus (N-KRAB) or carboxyl-terminus (C-KRAB) of SadCas9. The N-KRAB construct was more effective than C-KRAB at decreasing levels of both vimentin and Pcsk9. Thus, N-KRAB was chosen as the model CRISPRi construct but we cannot rule out the possibility that C-KRAB provides better efficacy against other targets.

Both U6 and 7SK RNA promoters have been used to express sgRNA. Whereas we found that both provided similar results against *VIMEN-TIN* in human ARPE cells, there was a clear difference against *Pcsk9* in mouse AML-12 cells. This difference may be due to human versus

Table 2. Enhancers and Promoters Used to Express KRAB-SadCas9 (N-KRAB)

Name	Abbreviation	Size (bp)	Function
Individual Components			
Albumin	Alb	205	enhancer
Hepatitis B enhancer II	HBV	155	enhancer
α1-antitrypsin	AAT	162	promoter
mini CMV	mCMV	59	promoter
Combined Enhancer and Promoters			
Elongation factor 1α	EF-1α	271[a]	
	Alb-AAT	367[a]	
	Alb-mCMV	370[a]	
	HBV-AAT	332[a]	
	HBV-mCMV	285[a]	

[a]Size of Mlu1/EcoR1 insert in Sleeping Beauty and AAV plasmids.

mouse cells or cell types. Nonetheless, the U6 promoter appears to be an overall better choice for expression of sgRNA.

The biggest constraint for including all CRISPRi components into the 4.7 kb packaging limitation of AAV is the size of a promoter driving expression of N-KRAB. Based on our current results, the maximum size of the promoter is 370 bp. Mouse liver cell lines were used to compare the efficacy of several enhancer/promoters that are within this size constraint. The 675 bp hepatocyte-selective combination of the albumin-enhancer and α1-antitrypsin promoter (Ealb-Pa1AT)[13] was reduced in size to 370 bp (Alb-AAT). Our 205 bp Alb enhancer contains the functional elements of the larger 370 bp enhancer, whereas our 162 bp AAT promoter lacks the upstream AP-1 and C/EBP elements but contains the tissue-specific and downstream elements of the larger 305 bp promoter. The smaller Alb-AAT enhancer/promoter is likely less active than the larger Ealb-Pa1AT construct that displayed only 2-fold less luciferase activity relative to CMV from liver extracts.[13] We found that the Alb-AAT and EF-1α promoters produced 14-fold and 6-fold lower levels of N-KRAB mRNA, respectively, relative to CMV. However, the Alb-AAT and EF-1α promoters each produced a similar 5-fold decrease in Pcsk9 mRNA and secreted Pcsk9 as cells with the CMV promoter. These results establish that the Alb-AAT enhancer/promoter produced levels of N-KRAB that was sufficient for a maximal CRISPRi response in these cells.

AAV plasmids were packaged in AAV8 vectors to examine CRISPRi function in mouse livers. The first set of experiments were designed to compare doses of viruses to the levels of N-KRAB mRNA from livers. Mice were sacrificed 3 weeks after the injection, a time point with maximal reduction of serum Pcsk9 with the dual AAV system.[4] The results of these studies suggest that a dose of 2×10^{11} vg/mouse produced maximal or near-maximal levels of N-KRAB mRNA at the 3-week time point. At this dose, the Alb-AAT promoter generated 12-fold higher levels of N-KRAB mRNA relative to the EF-1A promoter,

establishing that the Alb-AAT promoter is significantly more efficacious than the EF-1α promoter in mouse livers.

The final experiments addressed levels of Pcsk9 mRNA from mouse livers and protein from sera. Mice were tail-injected with PBS or 2×10^{11} vg/mouse of AAV2/8 containing Alb-AAT with either gStop or Pcsk9 gRNA. Relative to the AAV.gStop virus, the AAV.Pcsk9 virus decreased levels of mRNA 32% and protein 27%. This is less than the 50% and 83% reductions in mRNA and protein, respectively, with the dual AAV system.[4] It should be noted that those experiments involved a 12 h fasting period before analysis. Glucagon signaling, which is elevated in fasting, has been shown to increase Pcsk9 protein turnover without affecting mRNA levels,[18] which may in part explain the difference in mRNA and protein levels that were obtained between the two studies. Nonetheless, liver cell lines with identical CRISPRi components as the AAV produced 80% reductions in both mRNA and protein. Although enhancer/promoter elements likely require further optimization for increased expression *in vivo*, our results clearly establish that a functional CRISPRi construct that decreases expression of an endogenous gene can be packaged in a single AAV. This will increase the efficacy of targeting clinically relevant genes, particularly in post-mitotic cells such as neurons (for review see Li and Samulski[5]).

## MATERIALS AND METHODS
Plasmid Construction
Plasmids were created with combinations of DNA digests (NEB enzymes, New England Biolabs, Ipswich, MA, USA), synthetic DNA from either IDT (Integrated DNA Technologies, Coralville, IA, USA) or Genewiz (South Plainfield, NJ, USA), and PCR with Q5 polymerase (NEB). DNA was sequenced at Genewiz. The AAV2 backbone plasmid was purchased from Cell Biolabs (San Diego, CA; #VPK-410). The ZsGreen plasmid was purchased from Takara Bio (Mountain View, CA; #632428) and PCR was used to remove the DR degradation domain. Plasmids obtained from Addgene include Sleeping Beauty SBtet-Neo (#60509)[11] and SB100X expression (#34879).[10] A humanized form of SadCas9 was obtained from plasmid #70703[19] and the Kpn1/Pci1 fragment containing U6:sgRNA and Bsa1(−) AmpR was obtained from plasmid #84040[20]. All relevant SB and AAV plasmids will be available at Addgene.

gRNA Sequences
We utilized the published gRNA sequence of mouse Pcsk9 referred to as gRNA2,[4] which is 5′-GAGGGAAGGGATACAGGCTGGA-3′. For human *VIMENTIN*, the sequence of gRNA C5 is 5′-ACGAA CGAGGGCGCGGTGGGT-3′. The 5′ "A" was changed from the genomic "G" to decrease the hairpin melting temperature. Both "A" and "G" are efficient U6 and 7SK transcription start sites.[21] The gStop sequence is 5′-GGAGACCAAG-GCAGTTTTTT-3′. The gRNA present in many vector backbones is referred to here as non-targeting (NT); 5′-GGAGACCACGGCAGGTC-TCA-3′.

Cells
Cell lines purchased from ATCC (Manassas, VA, USA) included human ARPE-19 (ATCC #CRL-2302) and mouse AML-12 (ATCC
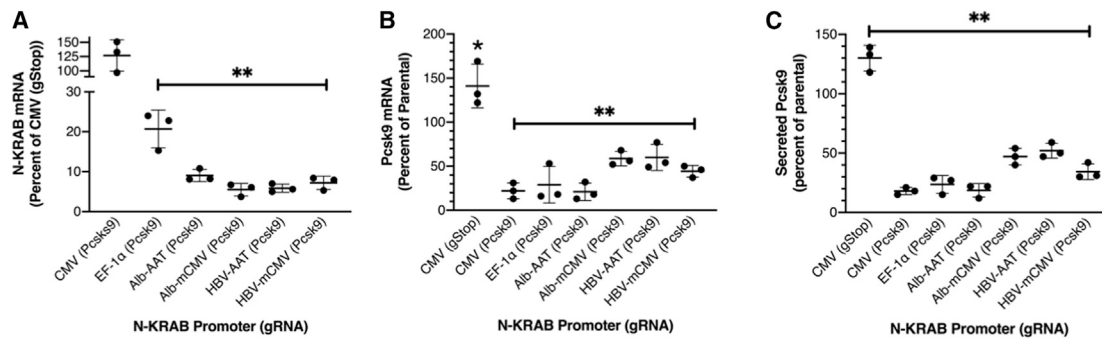
Figure 5. Comparison of Promoters Driving Expression of KRAB-SadCas9 (N-KRAB)

(A) Analysis of N-KRAB mRNA levels from the different promoters (see Table 2) relative to cells with CMV and U6:gStop. Levels of N-KRAB mRNA from the tested promoters were significantly lower than CMV (**p < 0.01). (B) *Pcsk9* mRNA levels and (C) Pcsk9 protein levels relative to parental AML-12 cells. The results (mean ± SD) are representative of three independent experiments. Asterisks denote significance at p < 0.05 (*) or p < 0.01 (**) relative to parental cells.

#CRL-2254). Both lines were grown in complete media consisting of DMEM/F12 (Thermo Fisher Scientific, Waltham, MA, USA; GIBCO #10565-018) supplemented with 15 mM HEPES (GIBCO #15630-080) and 10% (v/v) fetal bovine serum (GIBCO #26140-079). Confluent cultures were treated with TrypLE Express (GIBCO #12604) to passage cells.

Generation of Cell Lines

Cells at 50%–75% confluence in 6-well plastic plates were co-transfected with 1 µg each of SB SadCas9 and SB100X expression plasmids along with 8 µL FuGENE HD (Promega, Madison, WI, USA; #E2311). The transfection reagents were prepared in serum-free medium at a final volume of 200 µL and added to cells that were in 3 mL of complete media. After 2 days, media was replaced with fresh complete media containing G418 (Corning #30-234-CR) at either 1.0 mg/mL (AML-12 cells) or 1.5 mg/mL (ARPE-19). These concentrations provided 100% death of parental, non-transfected cells after 10–12 days of treatment.

Mouse Pcsk9 ELISA

Levels of Pcsk9 protein were determined from cultures of AML-12 cells or mouse sera. AML-12 cells in serum-free media became somewhat non-adherent on plastic and non-adherent on glass. Therefore, AML-12 cells and polyclonal cell lines were added to 6-well plastic plates that were coated with Geltrex (GIBCO #A15696-01). Each well was incubated with 1.2 mL Geltrex for 2 h at room temperature (RT). Wells were washed with PBS immediately before plating cells in complete media. The following day, wells were washed and replaced with 3 mL of serum-free media containing 2 or 5 µg doxycycline/mL (Sigma-Aldrich, St. Louis MO, USA; #D989) and incubated for 3 days. The lower concentration yielded similar results with less variability. For the experiments that compared CRISPRi activities of different promoters driving expression of KRAB-SadCas9 (e.g., CMV, Alb-AAT, or EF-1α), cells were not treated with doxycycline. Culture supernatant was collected, centrifuged at 17,000 × *g* for 15 min at 4°C, diluted 1:5 in assay buffer, and subjected to a mouse Pcsk9 Quantikine ELISA (R&D Systems, Minneapolis, MN, USA; cat-

alog # MPC900). Values were normalized to levels of total RNA. Mouse sera were diluted 1:20 in PBS immediately after collection and another 1:5 in assay buffer before analysis.

qPCR

RNA was isolated from cell lines and mouse livers. The procedure was identical for both sources except pieces of liver were placed directly into RNAprotect Tissue Reagent (QIAGEN GmbH, Hilden, Germany; #76106). Total RNA was isolated and separated from genomic DNA with an RNeasy Plus kit (QIAGEN #74124) according to the manufacturer's instructions. cDNA was prepared from 1 µg of RNA using an Applied Biosystems High Capacity cDNA Reverse Transcription kit (Thermo Fisher #4368814) according to the manufacturer's instructions. We used the same primers for mGAPDH and mPcsk9 as Thakore et al.[4] Primers for humanized SadCas9 were F: 5′-CGCATAGAGGAAATT-ATAAGAACAACCGG-3′ and R: 5′-TG AAGG-AATTGTCAAAGCTTACGGA-3′. qPCR of cDNA (2 µL) was performed with PerfeCTa SYBR Green FastMix ROX (Quantabio, Beverly, MA, USA; #84071) using Applied Biosystems QuantStudio 3 PCR system. Amplification conditions were 95°C for 10 min and 40 cycles of 95°C for 15 s and 60°C for 1 min. The Ct values of each target were normalized to Ct values of *Gapdh* to determine ΔCt, and fold-changes in target gene expression were calculated with the ΔΔCt method.

Antibodies

Mouse (#C15200230) and rabbit (#C15310260) antibodies against Sa Cas9 were purchased from Diagenode (Denville, NJ). The rabbit antibodies were diluted 1:1,000 for blots, 1:2,000 for immunocytochemistry of cell lines, and 1:1,000 for liver sections. Secondary fluorescent antibodies were obtained from Thermo Fisher. The remaining antibodies were purchased from Cell Signaling Technologies (Danvers, MA).

Immunoprecipitation

Cells in 10 cm plates were washed with PBS and then scraped and sonicated in 200 µL of PBS containing 2 Halt protease inhibitor
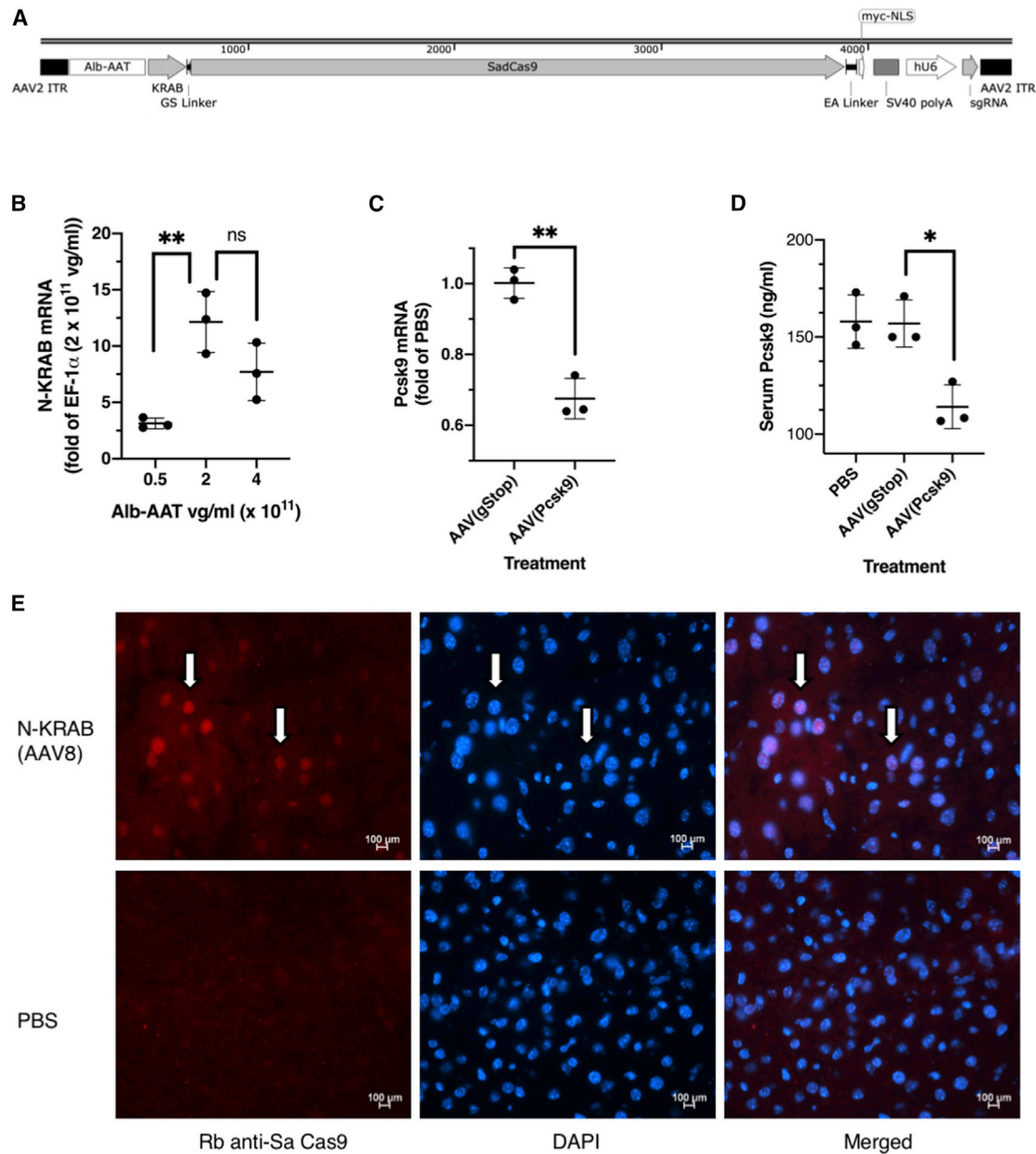
Figure 6. Analysis of a Single AAV CRISPRi that Targets *Pcsk9* in Mice

(A) Diagram of a representative AAV2 plasmid construct used to package AAV8.N-KRAB. The promoters included Alb-AAT or EF-1α (see Table 2) with either gStop or *Pcsk9* gRNA. (B) Fold-increase in N-KRAB mRNA from different doses of rAAV.N-KRAB.*Pcsk9* under control the Alb-AAT promoter relative to the EF-1α promoter at a dose of 2×10^{11} vg/mouse. The results are from one experiment and asterisks (**) denote $p < 0.01$. Mice tail-injected with PBS or Alb-AAT viruses with either gStop or *Pcsk9* gRNA at doses of 2×10^{11} vg/mouse were evaluated for (C) levels of *Pcsk9* mRNA relative to control PBS mice and (D) concentration of Pcsk9 from sera. The results presented in (C) and (D) are representative of two independent experiments and asterisks denote $p < 0.05$ (*) or $p < 0.01$ (**). (E) Immunolabeling of liver sections from mice treated with either 2×10^{11} vg/mouse of AAV8.N-KRAB (*Pcsk9*; top panels) or PBS (bottom panels). Sections were labeled with rabbit anti-Sa Cas9 (left panels) and DAPI (middle panels). The arrows denote nuclear labeling of N-KRAB. The results are representative of three animals from each treatment.

(Thermo Scientific #78430). PBS-soluble protein was collected after a $17,000 \times g$ spin for 15 min at 4°C. Protein concentrations were determined with the Bicinchoninic acid (BCA) protein assay (Thermo Scientific) using BSA as the protein standard. For immunoprecipitations,

2 μL of 10% Triton X-100 in PBS (to decrease surface tension) and primary antibody was added to 200 μg of protein in a final volume of 200 μL. The antibodies included mouse anti-Sa Cas9 (1 μg) or mouse anti-FLAG (2 μL). After 1 h at RT, 10 μL of anti-mouse beads

(Cell Signaling Technologies, Danvers, MA, USA; #5946) was added and incubated overnight at 4°C with shaking. Beads were washed twice with 1 mL of PBS containing 0.1% Triton X-100, treated with 50 μL of 1X SDS sample buffer (Bio-Rad, Hercules, CA, USA; #1610747) containing 2.5% 2-mercaptoethanol (Bio-Rad; #1610710), and heated at 70°C for 10 min.

Immunoblots

Proteins were electrophoresed in 4%–20% or 7.5% TGX gels (Bio-Rad) along with 5 μL or 10 μL, respectively, of SeeBlue Plus2 protein markers (Invitrogen/Thermo Fisher). Protein was transferred to 0.4 μm nitrocellulose membranes (Bio-Rad) in Tris/Glycine buffer without methanol at 100V for Δ+120mA (~15 min). Membranes were blocked with 2% BSA in TBS overnight at 4°C. Primary antibodies were incubated for 2 h at RT and secondary antibodies (alkaline phosphatase-conjugated, Jackson ImmunoResearch) for 1 h at RT. Blots were developed with NBT and BCIP (Pierce/Thermo Fisher).

Immunocytochemistry

Cells were grown in 8-well Lab Tek II chamber slides (Thermo Fisher; #154941). Slides for AML-12 cells were pre-coated with 80 μL of Geltrex as described above (Mouse Pcsk9 ELISA). Cells were fixed for 15 min in formaldehyde solution (Sigma-Aldrich; #F1635) diluted 1:10 in PBS, washed with TBS, and then permeabilized with 0.25% Triton X-100 in TBS for 15 min. Non-specific sites were blocked overnight at 4°C with TBS containing 2% immunoglobulin G (IgG)-free BSA (Jackson ImmunoResearch Laboratories, West Grove, PA; #001-000-161). Wells were incubated with primary and secondary antibodies diluted in TBS/1% IgG-free BSA. Fluorescent secondary antibodies were used at a dilution of 1:1,000. Coverslips were mounted with ProLong Gold with 4',6-diamidino-2-phenylindole (DAPI) (Thermo Fisher; #P36941).

AAV8 Mice Experiments

Plasmids were packaged in AAV8 particles and quantitated (vg/mL) at SignaGen Laboratories (Rockville, MD, USA). Quantitation was determined from qPCR of the SV40 pA. Male C57BL/6 mice were purchased from Jackson Laboratories (Bar Harbor, ME). Mice at 6–8 weeks of age were anesthetized with 1.5% isoflurane and secured into a chamber exposing the tail. A single tail vein injection of 200 μL AAV solution (5×10^{10}, 2×10^{11}, or 4×10^{11} vg in PBS) or sterile PBS was administered using a 26G needle. 3 weeks later, mice were euthanized and blood was collected by cardiac puncture prior to collection of liver tissue that was stored in RNAprotect Tissue Reagent (QIAGEN). Whole blood was allowed to clot in Z tubes (Greiner Bio-one, Kremsmunster, Austria; #450470) by leaving it undisturbed at RT. The clot was removed by centrifuging at 1,000–2,000 × g for 10 min in a refrigerated centrifuge. Approximately 100 μL of serum was collected per mouse and 10 μL immediately diluted 1:20 in PBS for the Pcsk9 ELISA. All procedures were performed in accordance with the VUMC Institutional Animal Care and Use Committee approved protocol and Association for Research in Vision and Ophthalmology guidelines.

Immunohistochemistry

Frozen chunks of mouse liver were embedded in OCT and cryo-sectioned at a thickness of 7 microns. Slides were air-dried for 30 min at RT and stored at −80°C. Tissues were fixed and permeabilized as per the immunocytochemistry protocol (above) and blocked with 5% (v/v) normal donkey serum (NDS, Jackson ImmunoResearch; #017-000-121) in PBS for 1–3 days at 4°C. Sections were labeled with rabbit anti-Sa Cas9 (1:1,000 in 2% NDS) overnight at 4°C. Sections were washed with PBS and labeled with donkey anti-rabbit antibodies conjugated to Alexa 594 (1:200 in 1% NDS) and incubated for 2 h. Sections were washed twice with PBS, once with water, and air-dried. Coverslips were mounted with VECTASHIELD antifade mounting medium with DAPI (Vector Laboratories, Burlingame, CA; #H-1200).

Statistics

All statistical analysis was performed using GraphPad Prism 8. All experimental conditions that involved statistics were performed with three technical replicates. For the cell culture studies involving trafficking of SadCas9, at least 250 Cas9-positive cells were analyzed for each construct per experiment and one-way ANOVA was performed followed by the Dunnett post hoc test. For the mice experiments, three mice per condition were analyzed and one-way ANOVA was performed followed by the Tukey post hoc test. All other statistical analyses were performed with an unpaired Student's t test.

AUTHOR CONTRIBUTIONS

Conceptualization, T.S.R.; Methodology, J.R.B.; Validation, J.R.B., J.S.; Formal Analysis, T.S.R., J.R.B.; Investigation, J.R.B., J.S., A.B.-C., M.C.W.; Resources, T.S.R.; Writing, original draft, J.R.B.; Writing, review & editing, T.S.R., J.R.B., J.S., A.B.-C., M.C.W.; Visualization, T.S.R., J.R.B.; Supervision, T.S.R.; Project Administration, T.S.R.; Funding Acquisition, T.S.R.

CONFLICTS OF INTEREST

The authors declare no competing interests.

the results are contained in the manuscript. Relevant AAV and Sleeping Beauty plasmids will be deposited at Addgene.

REFERENCES

1. Bellefroid, E.J., Poncelet, D.A., Lecocq, P.J., Revelant, O., and Martial, J.A. (1991). The evolutionarily conserved Krüppel-associated box domain defines a subfamily of eukaryotic multifingered proteins. Proc. Natl. Acad. Sci. USA *88*, 3608–3612.

2. Margolin, J.F., Friedman, J.R., Meyer, W.K.-H., Vissing, H., Thiesen, H.-J., and Rauscher, F.J., 3rd (1994). Krüppel-associated boxes are potent transcriptional repression domains. Proc. Natl. Acad. Sci. USA *91*, 4509–4513.

3. Witzgall, R., O'Leary, E., Leaf, A., Önaldi, D., and Bonventre, J.V. (1994). The Krüppel-associated box-A (KRAB-A) domain of zinc finger proteins mediates transcriptional repression. Proc. Natl. Acad. Sci. USA *91*, 4514–4518.

4. Thakore, P.I., Kwon, J.B., Nelson, C.E., Rouse, D.C., Gemberling, M.P., Oliver, M.L., and Gersbach, C.A. (2018). RNA-guided transcriptional silencing in vivo with *S. aureus* CRISPR-Cas9 repressors. Nat. Commun. *9*, 1674–1682.

5. Li, C., and Samulski, R.J. (2020). Engineering adeno-associated virus vectors for gene therapy. Nat. Rev. Genet. *21*, 255–272.

6. Lau, C.-H., Ho, J.W.-T., Lo, P.K., and Tin, C. (2019). Targeted transgene activation in the brain tissue by systemic delivery of engineered AAV1 expressing CRISPRa. Mol. Ther. Nucleic Acids *16*, 637–649.

7. Marqusee, S., and Baldwin, R.L. (1987). Helix stabilization by Glu$^-$...Lys$^+$ salt bridges in short peptides of *de novo* design. Proc. Natl. Acad. Sci. USA *84*, 8898–8902.

8. Nishimasu, H., Cong, L., Yan, W.X., Ran, F.A., Zetsche, B., Li, Y., Kurabayashi, A., Ishitani, R., Zhang, F., and Nureki, O. (2015). Crystal structure of *Staphylococcus aureus* Cas9. Cell *162*, 1113–1126.

9. Ivics, Z., Hackett, P.B., Plasterk, R.H., and Izsvák, Z. (1997). Molecular reconstruction of *Sleeping Beau*ty, a *Tc1*-like transposon from fish, and its transposition in human cells. Cell *91*, 501–510.

10. Mátés, L., Chuah, M.K., Belay, E., Jerchow, B., Manoj, N., Acosta-Sanchez, A., Grzela, D.P., Schmitt, A., Becker, K., Matrai, J., et al. (2009). Molecular evolution of a novel hyperactive *Sleeping Beauty* transposase enables robust stable gene transfer in vertebrates. Nat. Genet. *41*, 753–761.

11. Kowarz, E., Löscher, D., and Marschalek, R. (2015). Optimized Sleeping Beauty transposons rapidly generate stable transgenic cell lines. Biotechnol. J. *10*, 647–653.

12. Gao, Z., Herrera-Carrillo, E., and Berkhout, B. (2018). Delineation of the exact transcription termination signal for type 3 polymerase III. Mol. Ther. Nucleic Acids *10*, 36–44.

13. Kramer, M.G., Barajas, M., Razquin, N., Berraondo, P., Rodrigo, M., Wu, C., Qian, C., Fortes, P., and Prieto, J. (2003). *In vitro* and *in vivo* comparative study of chimeric liver-specific promoters. Mol. Ther. *7*, 375–385.

14. Kleinstiver, B.P., Prew, M.S., Tsai, S.Q., Topkar, V.V., Nguyen, N.T., Zheng, Z., Gonzales, A.P., Li, Z., Peterson, R.T., Yeh, J.R., Aryee, M.J., et al. (2015). Engineered CRISPR-Cas9 nucleases with altered PAM specificities. Nature *523*, 481–485.

15. Ran, F.A., Cong, L., Yan, W.X., Scott, D.A., Gootenberg, J.S., Kriz, A.J., Zetsche, B., Shalem, O., Wu, X., Makarova, K.S., et al. (2015). *In vivo* genome editing using *Staphylococcus aureus* Cas9. Nature *520*, 186–191.

16. Melén, K., Kinnunen, L., Fagerlund, R., Ikonen, N., Twu, K.Y., Krug, R.M., and Julkunen, I. (2007). Nuclear and nucleolar targeting of influenza A virus NS1 protein: striking differences between different virus subtypes. J. Virol. *81*, 5995–6006.

17. Mekhail, K., Rivero-Lopez, L., Al-Masri, A., Brandon, C., Khacho, M., and Lee, S. (2007). Identification of a common subnuclear localization signal. Mol. Biol. Cell *18*, 3966–3977.

18. Spolitu, S., Okamoto, H., Dai, W., Zadroga, J.A., Wittchen, E.S., Gromada, J., and Ozcan, L. (2019). Hepatic glucagon signaling regulates PCSK9 and low-density lipoprotein cholesterol. Circ. Res. *124*, 38–51.

19. Kleinstiver, B.P., Prew, M.S., Tsai, S.Q., Nguyen, N.T., Topkar, V.V., Zheng, Z., and Joung, J.K. (2015). Broadening the targeting range of *Staphylococcus aureus* CRISPR-Cas9 by modifying PAM recognition. Nat. Biotechnol. *33*, 1293–1298.

20. Ye, L., Wang, J., Tan, Y., Beyer, A.I., Xie, F., Muench, M.O., and Kan, Y.W. (2016). Genome editing using CRISPR-Cas9 to create the HPFH genotype in HSPCs: An approach for treating sickle cell disease and β-thalassemia. Proc. Natl. Acad. Sci. USA *113*, 10661–10665.

21. Gao, Z., Harwig, A., Berkhout, B., and Herrera-Carrillo, E. (2017). Mutation of nucleotides around the +1 position of type 3 polymerase III promoters: The effect on transcriptional activity and start site usage. Transcription *8*, 275–287.